Experimental investigation of the neutral sheet profile during magnetic reconnection*

Masaaki Yamada,[†,a)] Hantao Ji, Scott Hsu, Troy Carter, Russell Kulsrud, and Fedor Trintchouk
Princeton Plasma Physics Laboratory, P. O. Box 451, Princeton, New Jersey 08543

During magnetic reconnection, a ''neutral sheet'' current is induced, heating the plasma. The resultant plasma thermal pressure forms a stationary equilibrium with the opposing magnetic fields. The reconnection layer profile holds significant clues about the physical mechanisms which control reconnection. In the Magnetic Reconnection Experiment [M. Yamada *et al.*, Phys. Plasmas **4**, 1936 (1997)], a quasi steady-state and axisymmetric neutral sheet profile has been measured precisely using a magnetic probe array with spatial resolution equal to one quarter of the ion gyro-radius. It was found that the reconnecting field profile fits well with a Harris-type profile [E. G. Harris, Il Nuovo Cimento **23**, 115 (1962)], $B(x) \sim \tanh(x/\delta)$. This agreement is remarkable since the Harris theory does not take into account reconnection and associated electric fields and dissipation. An explanation for this agreement is presented. The sheet thickness δ is found to be ~ 0.4 times the ion skin depth, which agrees with a generalized Harris theory incorporating nonisothermal electron and ion temperatures and finite electric field. The detailed study of additional local features of the reconnection region is also presented. © *2000 American Institute of Physics.* [S1070-664X(00)95505-8]

I. INTRODUCTION

Magnetic reconnection,[1] the topological rearrangement of magnetic field lines, is a basic plasma phenomena of wide-ranging importance. It plays a major role in the evolution of solar flares[2] and in the interaction of the solar wind with the earth's magnetosphere,[3] and it often plays a dominant role in determining the confinement characteristics of high-temperature fusion plasmas.[4] Recent detailed data from laboratory plasma experiments, satellite observations, theoretical analysis, and computer simulations have advanced the understanding of magnetic reconnection both in space and laboratory plasmas.

The reconnection layer, often called the neutral sheet, is a focal point of reconnection research since magnetohydrodynamics (MHD) breaks down locally in the layer, while globally, the plasma has large Lundquist number and is approximated well by ideal MHD. Precise measurements of the neutral sheet profile can provide important clues to help understand the physical mechanisms of reconnection. Thanks to significant progress in data acquisition technology in the past two decades, the detailed magnetic field structure of the neutral sheet has been measured in laboratory plasmas. Extensive data have been accumulated in highly conductive MHD plasmas with large Lundquist numbers $S = 10 - 1000$, where S is the ratio of the magnetic diffusion time to the Alfvén transit time.

MRX[5] (Magnetic Reconnection Experiment) was built in 1995 at the Princeton Plasma Physics Laboratory for the comprehensive study of magnetic reconnection in a controlled environment. It has generated much fundamental data on magnetic reconnection in MHD plasmas. Our experiment has already addressed important issues related to the reconnection layer. Based on detailed magnetic field measurements by high-resolution magnetic probes, evolution of poloidal flux contours were deduced, demonstrating important two-dimensional (2D) features of magnetic reconnection.[6] The reconnection rate was also seen to agree with a generalized Sweet–Parker model.[7,8]

Generally, analysis of magnetic reconnection is divided into local and global issues. In local treatments, the reconnection rate is determined by local plasma parameters in the reconnection region. In these analyses, boundaries are not specified and boundary conditions are often replaced by initial conditions for plasma flow velocity. In global treatments, on the other hand, the reconnection rate is considered to be influenced or determined by the three-dimensional (3D) topology of the plasma configuration. Boundaries are well defined and the conservation of total flux or helicity is often discussed. Three dimensional MHD modes are often involved, and particle acceleration in all three dimensions are possible. The present paper addresses the most fundamental local reconnection physics issues by studying the features of the reconnection layer in MRX.

As magnetic field lines break and reconnect around the neutral layer, a current sheet is generated, heating the plasma. The plasma thermal pressure then forms an equilibrium with the magnetic pressure of the opposing magnetic field. While MHD can be used to treat the plasma globally, more general theories are necessary for a proper treatment of the neutral layer, where MHD breaks down. An important

question is what determines the profile of the reconnection layer. Harris[9] found analytical one-dimensional (1D) solutions for the magnetic field, plasma pressure, current density, and sheet thickness of a collisionless current sheet by solving the Vlasov–Maxwell equations with three important assumptions: (1) No electric field; (2) electrons and ions drifting in opposite directions at the diamagnetic speed; and (3) equal and spatially uniform electron and ion temperatures. The Harris solution is an elegant description of a neutral sheet and, therefore, is referenced very often in reconnection research. Numerical simulations have yielded[10–13] favorable comparisons with the Harris sheet, showing that the sheet thickness being equal to the ion skin-depth.[13] However, to our knowledge, the Harris sheet has not been previously investigated experimentally. The precise determination of magnetic field profiles in MRX now enables a detailed study of the current sheet thickness as a function of relevant parameters, which is the subject of this paper.

The paper is organized as follows. Section II presents a generalized theory of the Harris collisionless neutral sheet. Section III describes the experimental apparatus of MRX. Section IV presents detailed experimental results of the neutral sheet profile during reconnection. Section V concludes the paper with a summary and discussion.

II. THEORY OF A GENERALIZED HARRIS SHEET

A steady-state, collisionless current sheet can be analyzed using the steady-state Vlasov–Maxwell system of equations

$$\mathbf{v}\cdot\frac{\partial f}{\partial \mathbf{r}}+\frac{q}{m}(\mathbf{E}+\mathbf{v}\times\mathbf{B})\cdot\frac{\partial f}{\partial \mathbf{v}}=0,\tag{1}$$

$$\nabla\times\mathbf{E}=0,\tag{2}$$

$$\nabla\cdot\mathbf{E}=\frac{e}{\epsilon_0}\left(\int f_i d\mathbf{v}-\int f_e d\mathbf{v}\right),\tag{3}$$

$$\nabla\times\mathbf{B}=e\mu_0\left(\int \mathbf{v}f_i d\mathbf{v}-\int \mathbf{v}f_e d\mathbf{v}\right),\tag{4}$$

$$\nabla\cdot\mathbf{B}=0,\tag{5}$$

where $\mathbf{E}$ is the electric field, $\mathbf{B}$ the magnetic field, $\mathbf{v}$ the particle velocity, and f_i (f_e) the ion (electron) distribution function. In general, the equations are nonlinear and can only be solved numerically. However, E. G. Harris[9] derived a 1D steady-state analytical solution with specific assumptions. Below, we re-derive the Harris solution, relaxing a few of the original assumptions.

All solutions of Eq. (1) must be a function of the constants of the motion, i.e., the total energy $W\equiv mv^2/2\pm e\phi$ and the canonical momentum in the y and z directions, $p_y\equiv mv_y\pm eA_y$ and $p_z\equiv mv_z$, respectively. Here, ϕ is the electrostatic potential and the vector potential $\mathbf{A}$ is assumed to have only a y component A_y. Consider the distribution function

$$f=n_0\left(\frac{m}{2\pi T}\right)^{3/2}\exp\left\{-\frac{m[v_x^2+(v_y-V)^2+v_z^2]}{2T}\right.$$
$$\left.\pm\frac{e(VA_y-\phi)}{T}\right\},\tag{6}$$

where the constant, $T=T_e$ (T_i), is the electron (ion) temperature and the constant, $V=V_e$ (V_i), is the electron (ion) drift speed in the y direction. Because the argument of the exponential can be written as $(-W+p_yV-mV^2/2)/T$, f is a function of the constants of the motion and, therefore, a solution of Eq. (1). Harris realized that this shifted Maxwellian is the most natural solution. Here, we relax Harris' assumptions $T_e=T_i$ and $V_i=-V_e$.

In this 1D model, all variables are assumed to vary only in x, and T_i, T_e, V_i, and V_e are all assumed to be constant. The y direction is the direction of the current. The system of equations can be simplified significantly by assuming that $\mathbf{E}$ has only an x component $E_x=-\partial\phi/\partial x$. And since A_y is assumed to be the only nonzero component of $\mathbf{A}$, $\mathbf{B}$ has only a z component $B_z=\partial A_y/\partial x$. It should be noted that $E_y=0$ and the collisionless assumptions mean that there is no dissipation and hence no reconnection in this model.

Substitution of Eq. (6) into Eqs. (3) and (4) yields two coupled nonlinear differential equations for ϕ and A_y,

$$\frac{\partial^2\phi}{\partial x^2}=-\frac{en_0}{\epsilon_0}\left\{\exp\left[\frac{e(V_iA_y-\phi)}{T_i}\right]\right.$$
$$\left.-\exp\left[\frac{-e(V_eA_y-\phi)}{T_e}\right]\right\},\tag{7}$$

$$\frac{\partial^2A_y}{\partial x^2}=-en_0\mu_0\left\{V_i\exp\left[\frac{e(V_iA_y-\phi)}{T_i}\right]\right.$$
$$\left.-V_e\exp\left[\frac{-e(V_eA_y-\phi)}{T_e}\right]\right\}.\tag{8}$$

By using normalized variables $\hat{\phi}\equiv e\phi/T_e$ and $\hat{x}\equiv x/(c/\omega_{\mathrm{pi}})$ (where $\omega_{\mathrm{pi}}\equiv n_0e^2/\epsilon_0m_i$ is the ion plasma frequency), Eq. (7) is cast into dimensionless form

$$\frac{\partial^2\hat{\phi}}{\partial\hat{x}^2}=-\left(\frac{c/\omega_{\mathrm{pi}}}{\lambda_D}\right)^2\left\{\exp\left[\frac{e(V_iA_y-\phi)}{T_i}\right]\right.$$
$$\left.-\exp\left[\frac{-e(V_eA_y-\phi)}{T_e}\right]\right\},\tag{9}$$

where the left-hand side (LHS) is of order unity but $(c/\omega_{\mathrm{pi}}/\lambda_D)^2$ is of order 10^6 (λ_D is the Debye length in MRX). Therefore, quasineutrality $\{\cdots\}\simeq0$ must be satisfied, leading to an ambipolar potential

$$\phi=\frac{T_eV_i+T_iV_e}{T_e+T_i}A_y.\tag{10}$$

Interestingly, ϕ is proportional to A_y. Substituting Eq. (10) into Eq. (8) gives a nonlinear equation in only A_y

$$\frac{\partial^2 A_y}{\partial x^2} = -en_0\mu_0(V_i-V_e)\exp\left[\frac{e(V_i-V_e)}{T_e+T_i}A_y\right]. \quad (11)$$

With appropriate boundary conditions, this equation can be solved analytically, yielding modified Harris solutions

$$A_y = -\delta B_0 \log\cosh\left(\frac{x}{\delta}\right), \quad (12)$$

$$B_z = -B_0 \tanh\left(\frac{x}{\delta}\right), \quad (13)$$

$$j_y = \frac{B_0}{\mu_0\delta}\mathrm{sech}^2\left(\frac{x}{\delta}\right), \quad (14)$$

$$E_x = \frac{T_eV_i+T_iV_e}{T_e+T_i}B_0\tanh\left(\frac{x}{\delta}\right), \quad (15)$$

$$p = n_0(T_e+T_i)\mathrm{sech}^2\left(\frac{x}{\delta}\right), \quad (16)$$

where $B_0^2/(2\mu_0)=n_0(T_e+T_i)$. The current sheet thickness δ is given by

$$\delta = \frac{c}{\omega_{\mathrm{pi}}}\frac{\sqrt{2(T_e+T_i)/m_i}}{V_i-V_e} = \frac{c}{\omega_{\mathrm{pi}}}\frac{\sqrt{2}V_s}{V_{\mathrm{drift}}}, \quad (17)$$

where $V_s \equiv \sqrt{(T_e+T_i)/m_i}$ and $V_{\mathrm{drift}} \equiv V_i-V_e$ is the relative drift between ions and electrons. It should be noted that the above solution is more general than the original Harris solution, which is limited to $E_x=\phi=0$. The original Harris solution can be recovered by setting $T_e=T_i=T$ and $V_i=-V_e=V$ in Eq. (17) which yield $\delta=(c/\omega_{\mathrm{pi}})(\sqrt{T/m_i}/V)$.

Since the Harris solution is only one of many which might be obtained by choosing f as a function of the constants of the motion (albeit the one most easily solved analytically), one might ask why the experiment ''selects'' the Harris profile. A possible explanation might the following. In the experiment, the ion crossing time of the layer, which is equal to the ion cyclotron time since the thickness of the layer is approximately one ion gyro-radius, and the ion–ion collision time are much shorter than the time the plasma takes to flow through the layer. As a result, the ions should be in an equilibrium state, neglecting the reconnection velocity V_x. Furthermore, as confirmed by experiment, they are isothermal across the layer, satisfying the full Vlasov–Fokker–Planck equation. Now the Harris solution satisfies the Vlasov equation as discussed above. However, it is a shifted Maxwellian solution, Eq. (6), which makes the ion–ion Fokker–Planck term vanish, and it is probably the only solution of the Vlasov equation which does this. As a result, the ion current is proportional to an exponential in A_y, the first term in Eq. (8).

The ion current is really a diamagnetic current proportional to $T_i(\partial n/\partial x)/nB$ for constant T_i. If the electron temperature is also constant, then its current is proportional to $T_e(\partial n/\partial x)/nB$ and thus also proportional to an exponential in A_y. Hence, under the assumption of constant T_e and constant T_i in the layer, as measured in MRX, one should expect to get the Harris profile for B.
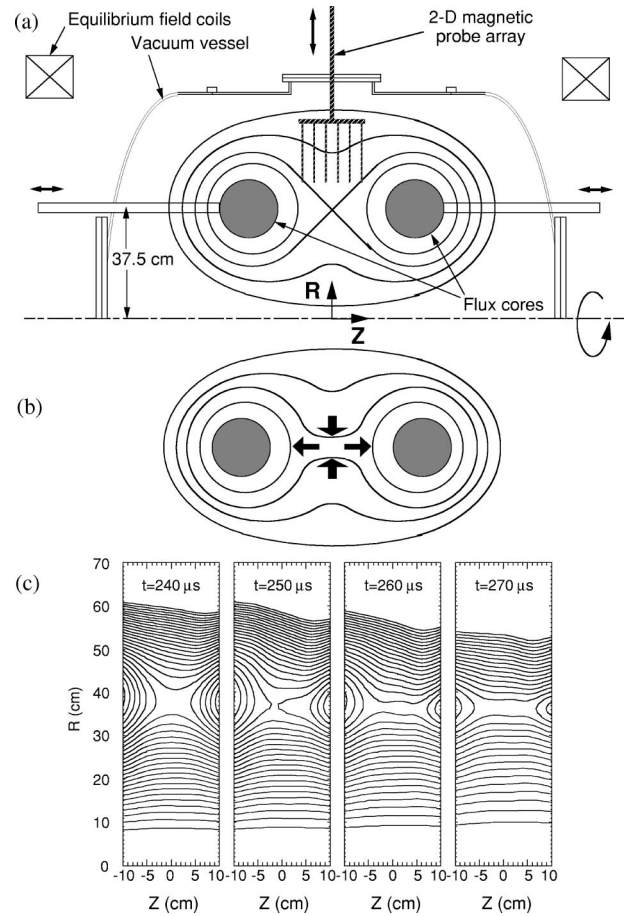

FIG. 1. (a) Experimental setup showing flux-cores and magnetic probe array. (b) Schematic of pull reconnection. (c) Time evolution of poloidal flux calculated from magnetic probe data, showing the development of a quasi steady-state neutral sheet.

We note that it cannot be argued that the electron distribution is *necessarily* a shifted Maxwellian (or even a solution of the Vlasov equation) since frictional electron–ion collisions would distort such a shifted Maxwellian. However, this distortion is small and should not modify the electron current from being proportional to the exponential in A_y. Therefore, it does not affect the Harris solution, i.e., Eqs. (7) and (8) hold. At the same time, the electron–ion collision integral gives rise to the resistivity term ηj_y. This term is balanced by an induced electric field E_y which produces an additional x directed flow, V_x, bringing magnetic field lines into the layer to be reconnected. (Taking the V_y moment of the Fokker–Planck equation yields Ohm's law, $E_y+V_x \times B_z=m\nu_{ei}V_y/e=\eta j_y$.) However, the reconnection time scale (δ/V_x) is much longer than the dynamical time scale (the ion crossing time). Therefore, the finite resistivity term introduces only a higher-order correction to the Harris solution. If the resistivity is anomalous, the remarks above still apply with the resistivity replaced by the anomalous resistivity.

The Harris model has been generalized further by S. M. Mahajan[14] to include time dependence, cylindrical geometry, and various density and velocity profiles. Generally, the solutions must be determined numerically. However, when
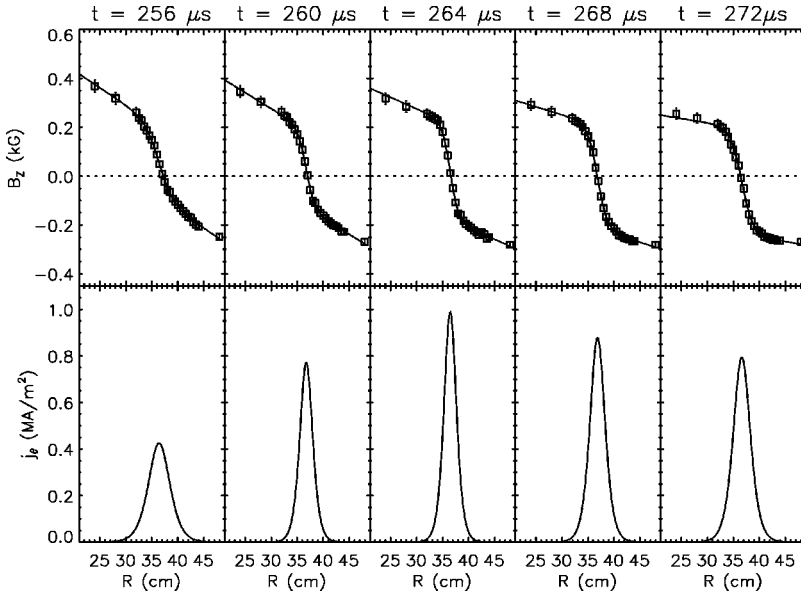
FIG. 2. Shown are reconnecting field (top) and current density (bottom) radial profiles taken in one plasma discharge. $B_Z(R)$ data are fit to the Harris sheet magnetic field profile modified by a background quadrupole field, Eq. (19), from which $j_\theta(R)$ is deduced, Eq. (20).

ions drift in the toroidal direction (y direction in Cartesian coordinates) with constant angular velocity $\omega = V_{i\theta}/r$, an analytical solution is found,[15] with

$$B_z = B_0 \tanh\left(\frac{r^2 - r_0^2}{r_0 \delta}\right), \tag{18}$$

where r_0 is the radial position of the center of the current sheet.

The ''Harris sheet'' solution is a simple analytical equilibrium solution for a plasma confined between oppositely directed magnetic fields. The convenient analytical expressions for the B_z, j_y, and p profiles and the sheet thickness δ lend themselves to direct comparisons with both computer simulations and experiments. However, it is important to keep in mind the limitations and assumptions of the Harris model, including the fact that it is 1D and does not include the effects of reconnection and associated electric fields, and to find out how reconnection and 2D effects modify the Harris equilibrium.

III. EXPERIMENTAL APPARATUS

Experiments for this research have been performed in the MRX device.[5] The attainable magnetic Lundquist number S is 300–1000. Figure 1(a) shows the present experimental setup in MRX. Two flux cores with 37.5 cm major radii and 9.4 cm minor radii are installed in the vacuum vessel. Inside each core, there is a four-turn, PF coil that carries toroidal current and a helical 36-turn toroidal solenoid (TF coil) that also acts as a one-turn toroidal current coil. By properly programming currents in the PF and TF coils, plasma current and toroidal field can be prescribed, independent of the sense of helicity in the toroidal solenoid. The coils are powered by two sets of capacitor banks, each of them containing eight 60 μF, 20 kV capacitors and 50–100 kJ of stored energy.

The present experiments are conducted in the double annular plasma setup, in which two toroidal plasmas with annular cross sections are formed independently around the

flux cores. Magnetic reconnection is then driven in the quadrupole field. By pulsing currents in the TF coils after a quadrupole poloidal magnetic field has been established by the PF coil currents, plasmas are created around each flux core due to inductive poloidal electric fields. At the same time, a common annular plasma forms outside the two inner plasmas surrounding each flux core. Thus, the magnetic field domain can be divided into a public domain and two private domains. Once the annular plasmas are created, the PF coil current can be increased or decreased. In the case of increasing PF coil current, the poloidal flux in each plasma is ''pushed'' toward the X-point (push mode). In the case of decreasing PF coil current, the poloidal flux in the public region is ''pulled'' back toward the x-point (pull mode), as illustrated in Fig. 1(b).

In the present MRX experiments, pull mode has been utilized without an magnetic axial field [the third vector component, in the toroidal direction θ in Fig. 1(a)]. In this so-called ''null-helicity'' reconnection, the direction of the field lines changes sharply at the reconnection point. Figure 1(c) shows the time evolution of measured poloidal flux contours during null-helicity reconnection. It should be noted that the pull mode geometry shares some common geometrical features with the plasma sheet at the magnetotail, in which time variation of the ring current and cross-tail currents induces magnetic reconnection, as well as with helmet streamer structures in the solar corona.

To document the internal magnetic structure of the reconnection in a single shot, two-dimensional magnetic probe arrays are placed in an R–Z plane, as shown in Fig. 1(a). Density and electron temperature T_e are measured using a triple Langmuir probe. Ion temperature T_i is estimated using Doppler spectroscopy of the H_β line, based on fast charge-exchange times on the order of 1 μs, and ion flows are measured using a Mach probe. Plasma parameters are as follows: $B \sim 0.5$–1.0 kG, $n_e \sim 0.1$–2.0×10^{14} cm^{-3}, $T_e \sim 5$–20 eV, and $T_i \sim 10$–30 eV.
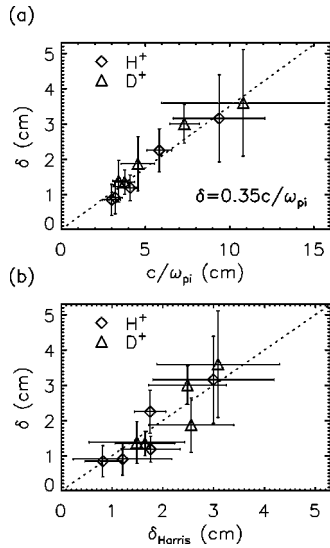
FIG. 3. Measured neutral sheet thickness δ vs (a) ion skin depth c/ω_{pi} and (b) vs theoretical Harris value given by Eq. (17).

IV. EXPERIMENTAL RESULTS

A. Measurement of neutral sheet profiles

It was found previously that driven reconnection in MRX generates an axisymmetric neutral sheet.[6] It is natural to ask whether the Harris equilibrium, which was derived as a 1D equilibrium between a confining magnetic field and plasma pressure, could be observed and whether the magnetic reconnection process would affect the neutral sheet profiles given in Eqs. (12)–(17).

Precise magnetic field profiles of the MRX neutral sheet have been measured by a high-resolution 1D magnetic probe array, which contains magnetic pickup coils every 5 mm, and is inserted radially across the neutral sheet. Figure 2 shows the time evolution of measured $B_Z(R)$ data, which are fitted to

$$B_Z(R) = -B_0 \tanh[(R-R_0)/\delta] + b_1 R + b_2, \qquad (19)$$

from which the current density j_θ is derived,

$$j_\theta(R) = \frac{B_0}{\mu_0 \delta} \mathrm{sech}^2[(R-R_0)/\delta]. \qquad (20)$$

The factors b_1 and b_2 are determined by the background quadrupole and equilibrium fields. The latter is applied to keep the plasma in a desirable position. The factor b_1 does not appear in Eq. (20) because it is canceled exactly by $\partial B_R/\partial Z$ of the background quadrupole field. Note that the MRX coordinates R, θ, and Z correspond to x, y, and z in the Harris model. Between $t \approx 260$ μs and $t \approx 275$ μs, the reconnection layer is maintained in quasi steady-state. It should be noted that, as reported previously,[5] the B_Z data also fit well to an arctangent, leading to a Lorentzian profile for j_θ. In our systematic studies, error functions (which lead to Gaussian j_θ) do not give as good a fit as either hyperbolic tangents or arctangents. Since this paper focuses on the physical picture of the Harris model, only hyperbolic tangent fitting is shown. The difference between using Eqs. (19) and (18) for fitting is negligible due to the large aspect ratio $R_0 \gg \delta$ in MRX.

The neutral sheet thickness δ can be determined accurately from the fit in Eqs. (19) and (20). By varying the discharge voltage and using both hydrogen and deuterium fill
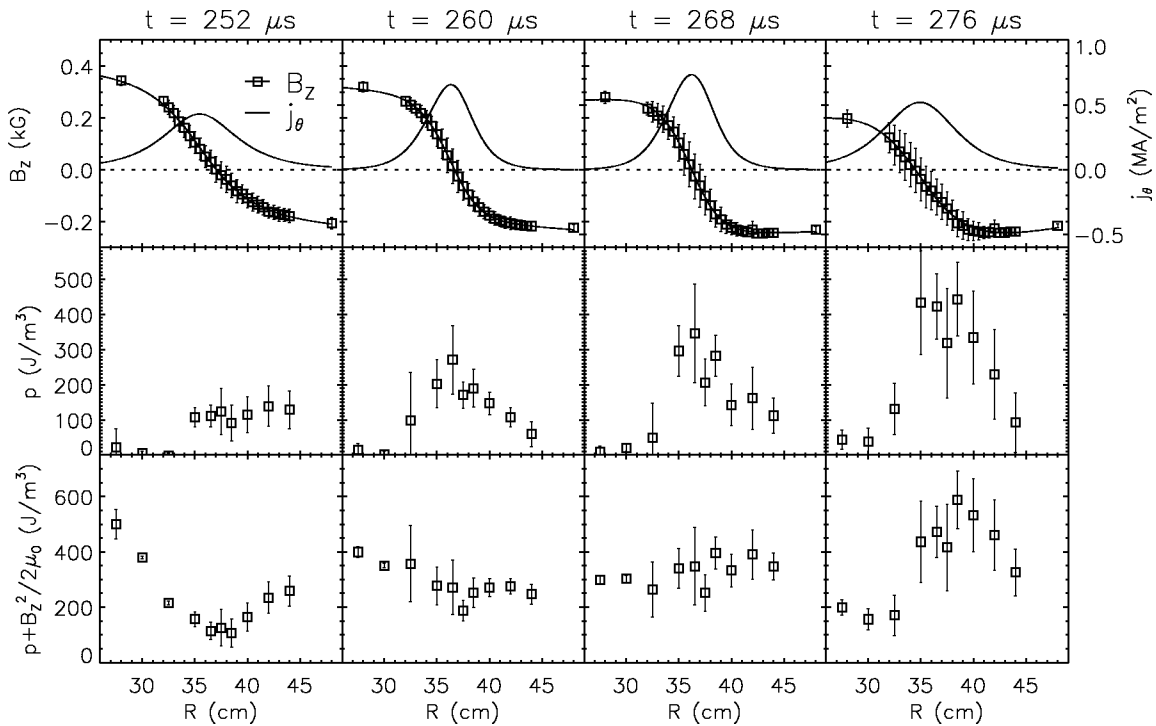

FIG. 4. Radial profiles of (top) reconnecting field and toroidal current density, (middle) plasma pressure, and (bottom) plasma thermal plus magnetic field pressure. Static equilibrium is maintained from $t \approx 260$–270 μs.

gas (to change the density and mass, respectively), a range of δ's and c/ω_{pi}'s were measured experimentally. Figure 3(a) shows that the data match well with $\delta \approx 0.35 c/\omega_{pi}$, i.e., δ scales with c/ω_{pi}. The modified Harris theory gives a prediction for δ_{Harris}, as given in Eq. (17). Experimentally, δ, c/ω_{pi}, and $\sqrt{2} V_s/V_{drift}$ are all determined independently, so we can compare δ versus δ_{Harris}. Figure 3(b) shows good agreement between δ and δ_{Harris}.

The 1D Harris solution should satisfy MHD force balance, $j_y B_z = \nabla p$, which simplifies to $p + B_z^2/2\mu_0$ = constant. Radial profiles of n_e and pressure $p = n(T_e + T_i)$ in MRX have been measured to check this static force balance. The radial profiles of $B_Z(R)$, $j_\theta(R)$ and $p(R)$ are shown in Fig. 4. The third row of Fig. 4 plots the radial profile of $p + B_Z^2/2\mu_0$, which shows that MHD force balance is satisfied during the central time of reconnection but not at the beginning or at the end of the reconnection phase. In the early phase of reconnection ($t \lesssim 255$ μs), magnetic pressure dominates the total pressure profile and reconnection drives low-beta plasma into the neutral sheet region. When plasma pressure increases to balance the magnetic pressure ($t \approx 255-272$ μs), equilibrium is established to maintain quasi steady-state reconnection. In the Sweet–Parker model, this situation is described as a steady flow of plasma frozen into the magnetic field from the R direction to the Z direction. In MRX, strong ion heating[16] and compressibility[7] create a state of excess kinetic pressure in the neutral sheet ($t \gtrsim 272$ μs), breaking the pressure balance.

The excellent fit of MRX magnetic data points to the Harris profile and the agreement between measured and predicted δ are remarkable since the MRX plasma is undergoing reconnection. However, based on the discussions in Sec. II regarding the effects of dissipation, the excellent agreement indicates that the Harris profile is the most natural one for a quasi steady-state reconnecting plasma sheet. Phenomenologically, since dissipation is related to an effective resistivity through Ohm's law along the current sheet, $\eta j_y = E_y - V_x B_z$, one expects that static equilibrium in the x direction (R in MRX) can be maintained during the reconnection process provided $V_x \ll V_A$, which is satisfied in MRX ($V_x/V_A \lesssim 0.1$).

The precise determination of the magnetic field profile in MRX has enabled a detailed study of the neutral sheet thickness δ as a function of other relevant parameters. It is found that $\delta \sim c/\omega_{pi}$. In anti-parallel reconnection cases in MRX, the ion gyro-radius ρ_i is on the order of c/ω_{pi}. This indicates the importance of pressure balance (between p and $B_0^2/2\mu_0$) and ion gyro-motion in determining the structure of reconnection region. This result is in rough agreement with numerical simulations[10–13] and observations in the geotail and the magnetopause.[3] The detailed features of the neutral sheet profile provide a good indicator for the nature of magnetic reconnection.

B. Enhanced ion heating and ion flows in the reconnection layer

One of the most important local physics issues for magnetic reconnection is how magnetic energy is converted into
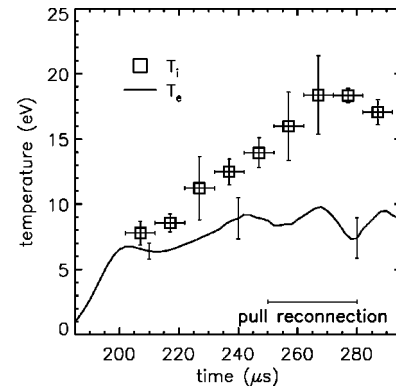

FIG. 5. Time evolution of global T_i (measured using Doppler spectroscopy in helium discharges) and T_e, showing fast ion heating.

plasma thermal energy. Figure 5 shows the time evolution of global T_i and local T_e during magnetic reconnection in helium discharges. These T_i measurements are based on chord-averaged Doppler spectroscopy of the He*II* 4686 Å line. Plasma light is collected along a sightline located in the plane $Z=0$ cm and tangent to the reconnection layer at $R = 37.5$ cm. It is seen that the average T_i rises initially together with T_e but later surpasses T_e by as much as a factor of three. It is difficult to obtain precise spectral measurements of T_i in hydrogen discharges, although the hydrogen data show very similar trends. Recently, local ion heating due to reconnection has been identified[16] in MRX using more rigorous measurements from a novel spectroscopy probe[17] placed inside the neutral sheet. These results are reported in detail elsewhere.[16] The significant ion heating was found to be much larger than the values predicted by classical dissipation.

Mach probe measurements show downstream ion flow along the neutral layer $V_{iZ}(Z)$ (for $R = 37.5$ cm), as shown in Fig. 6. Using an unmagnetized fluid sheath theory[18] generalized for $T_i \gtrsim T_e$, it is shown that the maximum $V_{iZ} \lesssim 0.2 V_A \approx 10$ km/s. The Mach probe measurements were calibrated using Doppler shifts obtained by the spectroscopy probe. The sub-Alfvénic flow is understood to result from high down-
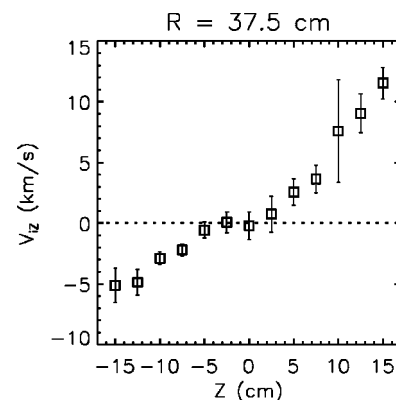

FIG. 6. Ion downstream flow speed along the neutral layer, as measured by a Mach probe, is established early during the reconnection phase, $t=250$ μs. The flow remains sub-Alfvénic throughout the quasi steady-state pull reconnection phase ($V_A \approx 60$ km/s).

stream pressure and moderate ∇p in the Z direction.[7] The flow speed is seen to increase linearly along the layer from $Z=0 \rightarrow 10$ cm. The peak flow velocity differs from classical MHD reconnection models, which predict Alfvénic ion outflows.

The observed enhanced ion heating cannot be due to thermalization of energetic flows. Instead, it is likely that the heating is caused by fluctuations which are also believed to play a dominant role in determining the plasma resistivity and ultimately the reconnection rate.

V. SUMMARY AND DISCUSSION

The neutral sheet profile during magnetic reconnection has been measured precisely in MRX. The magnetic field profile is seen to agree remarkably well with the Harris sheet profile even though the Harris theory does not take into account reconnection and associated dissipation. The measured neutral sheet thickness δ is seen to scale with the ion skin depth c/ω_{pi} according to $\delta \approx 0.4 c/\omega_{pi}$ over a wide range of discharge conditions. These results imply that that one can include the effects of quasi-steady state reconnection within the basic formulation of the Harris sheet. Because the shifted Maxwellian velocity distribution function satisfies the full Fokker–Planck equation (leaving out the small electron–ion collision term), it appears also to be the natural state for a reconnecting plasma.

It is also found that a static force balance is maintained between incoming magnetic field and the neutral sheet plasma pressure during the quasi-steady state phase of reconnection. Deviation from pressure balance occurs in the beginning and ending phases without changing the magnetic profile shape from that of the Harris solution. It was found[16] that a significant amount of magnetic energy is converted to thermal energy of the neutral sheet plasma during reconnection and that the energy conversion rate is much larger than the value expected from classical dissipation mechanisms. In earlier studies, it was found that a generalized Sweet–Parker model, which incorporates compressibility, downstream pressure and the effective resistivity, can explain the reconnection rate in MRX.[7,8]

A significant implication of the MRX results to date is that a stable 2D reconnection neutral sheet with axisymmetric geometry is consistent with both the Sweet–Parker and the Harris models with generalizations. Resistivity enhancement is observed during reconnection in the collisionless regime. Experimental measurements of the neutral sheet thickness δ agree well with our modified Harris theory for a nonisothermal plasma ($T_e \neq T_i$). The relationship $\delta \approx 0.4 c/\omega_{pi} \sim \rho_i$ suggests that V_{drift} is limited to a value equal to a constant on the order of 3 or 4 times the ion thermal speed.[8] These results lead us to suspect that a current-driven instability might be excited to limit the current. Immediate future efforts on MRX will be devoted to identifying the cause of the enhanced resistivity, including macro- and micro-instabilities.

[1] V. M. Vasyliunas, Rev. Geophys. Space Phys. **13**, 303 (1975).
[2] See, e.g., E. N. Parker, in *Cosmical Magnetic Fields* (Clarendon, Oxford, 1979).
[3] See, e.g., M. G. Kivelson and C. T. Russell, *Introduction to Space Physics* (Cambridge University Press, Cambridge, 1995).
[4] J. B. Taylor, Rev. Mod. Phys. **58**, 741 (1986).
[5] M. Yamada, H. Ji, S. Hsu, T. Carter, R. Kulsrud, N. Bretz, F. Jobes, Y. Ono, and F. Perkins, Phys. Plasmas **4**, 1936 (1997).
[6] M. Yamada, H. Ji, S. Hsu, T. Carter, R. Kulsrud, Y. Ono, and F. Perkins, Phys. Rev. Lett. **78**, 3117 (1997).
[7] H. Ji, M. Yamada, S. Hsu, and R. Kulsrud, Phys. Rev. Lett. **80**, 3256 (1998).
[8] H. Ji, M. Yamada, S. Hsu, R. Kulsrud, T. Carter, and S. Zaharia, Phys. Plasmas **6**, 1743 (1999).
[9] E. G. Harris, Nuovo Cimento **23**, 115 (1962).
[10] D. Biskamp, Phys. Fluids **29**, 1520 (1986).
[11] R. Horiuchi and T. Sato, Phys. Plasmas **1**, 3587 (1994).
[12] D. M. Uzdensky, Ph.D. Thesis, Princeton University (1998).
[13] M. A. Shay, J. F. Drake, R. E. Denton, and D. Biskamp, J. Geophys. Res. **103**, 9165 (1998).
[14] S. M. Mahajan, Phys. Fluids B **1**, 43 (1989).
[15] S. M. Mahajan and R. D. Hazeltine, ''Sheared flow generalization of the Harris sheet,'' accepted in Phys. Plasmas (2000).
[16] S. C. Hsu, G. Fiksel, T. A. Carter, H. Ji, R. M. Kulsrud, and M. Yamada, Phys. Rev. Lett. (to be published).
[17] G. Fiksel, D.J. D. Hartog, and P. W. Fontana, Rev. Sci. Instrum. **69**, 2024 (1998).
[18] M. Hudis and L. M. Lidsky, J. Appl. Phys. **41**, 5011 (1970).